Quantitative analysis of lake-cooling effect in Hefei, China, based on multispectral remote sensing and its response to urban expansion

Xuening Lin
Anhui Agricultural University
Yuhuan Cui (cuiyh@ahau.edu.cn)
Anhui Agricultural University
Shuang Hao
Anhui Agricultural University
Hong Hong
Anhui Agricultural University
Man Zhang
Anhui Agricultural University
Jingdong Zhang
Anhui Agricultural University
Ruonan Li
Anhui Agricultural University
Mengyu Liu
Anhui Agricultural University

Research Article

Keywords: lake-cooling efficiency, cooling intensity, cooling distance, urban lake, Hefei, China

Posted Date: April 13th, 2022

DOI: https://doi.org/10.21203/rs.3.rs-1499939/v1

Quantitative analysis of lake-cooling effect in Hefei, China, based on multispectral remote sensing and its response to urban expansion

Lin Xuening [a], Cui Yuhuan [a,b*], Hao Shuang [a,b], Hong Hong [a], Zhang Man [a], Zhang Jingdong [a], Li Ruonan [a], Liu Mengyu [a]

[a] School of Science, Anhui Agricultural University, Hefei, Anhui 230036, China

[b] Key Laboratory of Agricultural Sensors, Ministry of Agriculture and Rural Affairs of China, Hefei, Anhui 230036, China

Abstract: Urban expansion has intensified the heat-island effect, and the negative impact on the natural environment has gradually become considerable. However, urban lakes can significantly alleviate the heat-island effect caused by urbanization. Based on four-phase multispectral remote-sensing images during 2005–2020, 17 lakes in the main and surrounding urban areas of Hefei, China, were selected as the objects of our research. Each lake's cooling intensity and distance were calculated; cooling-efficiency data for different lakes were compared and analyzed considering lake areas and regional differences. The following conclusions were drawn: (1) The central temperature of the lakes correlated positively with cooling intensity ($R = 0.55$, $P < 0.01$) but negatively with cooling distance ($R = -0.28$, $P < 0.05$); the area of the lakes was significantly positively correlated with cooling distance ($R = 0.49$, $P < 0.01$) and weakly positively correlated with cooling intensity. When a lake area reached a certain threshold, its cooling intensity tended to stabilize. (2) The lakes around

the urban area were far away from the main urban area where the heat-island effect was most concentrated, the ability of absorbing the high surface temperature caused by the heat-island effect was limited, the cooling-intensity and cooling-distance efficiency were less than those of the main urban lakes. (3) With urban expansion and the intensified urban heat-island effect, the cooling-intensity efficiency of lakes in the main urban area gradually increased, whereas the cooling-distance efficiency of lakes decreased.

Keywords: lake-cooling efficiency; cooling intensity; cooling distance; urban lake; Hefei, China

1 Introduction

With the acceleration of global urbanization and the impact of climate change (Chen et al. 2021), the normal relationship between surface temperature and the atmosphere has been distorted, urban surface temperature has risen significantly, and the urban heat-island effect has continued to intensify (Wu et al. 2021; Zheng et al. 2022). The urban heat-island effect has serious negative impacts on human society (such as effects on the physical and mental health of urban residents) and brings a series of challenges to human survival (including massive consumption of energy and water) (Cai et al. 2018; Santamouris 2020; Wang 2022). These problems are closely related to the daily life of residents, including productivity and social interaction, and they also seriously violate the green principle of sustainable development of human society (Yao et al. 2022). To meet the above challenges, researchers and government departments have proposed a series of mitigation measures and solutions for the urban heat-island effect, among which the most-recognized measure is to improve the urban ecological space (Chen et al. 2019; Fan et al. 2017; Janhall 2015). The urban heat-island effect could be alleviated through adding and maintaining urban lakes (Douglas et al. 2019; Matos et al. 2019; von Schneidemesser et al. 2019), which would maximize the cooling effect of urban ecological space.

Lakes within cities have significant cooling and humidifying effects, which to a certain extent can reduce the temperature of wetlands and adjacent urban areas and can effectively regulate the urban microclimate such as by improving the urban thermal environment (Gunawardena et al. 2017). Mitigation of the urban heat-island effect through lakes is also widely considered to be environmentally friendly (Moss et al. 2019). Regarding the influence of the cooling efficiency of urban lakes, relevant research has focused mainly on the relationship between lakes and surface temperature (Cheval et al. 2020) and the effects of such factors as the spatial layout of lakes (including area, geometric shape, etc.) on cooling intensity (Ke et al. 2021), etc. However, the spatiotemporal heterogeneity of lake-cooling efficiency within the context of urban expansion and climate change has largely been ignored.

Therefore, for the research area, we selected Hefei (the capital city of Anhui Province in China), which is undergoing rapid urbanization, and we conducted research mainly involving three approaches: (1) On the basis of cooling intensity and distance, we quantitatively analyzed the cooling efficiency of lakes of various sizes and in different locations to reveal the relationship between lake area and cooling efficiency. (2) According to the distance from the lake to Hefei city center and the lake's spatial location, we divided the waterbodies into two types—those in the main urban area and those surrounding that area—and then separately analyzed the heterogeneity of their cooling efficiency. (3) We did comparative analyses of the response relationship of lake-cooling intensity and distance to urban expansion during 2005–2020.

The purpose of this study was both to understand the cooling efficiency of urban lakes and its influencing factors and to provide a theoretical basis for improving the urban heat-island effect and promoting sustainable urban development.

2 Data and methods

2.1 Overview of study area

Hefei (116°41′–117°58′E, 30°57′–32°32′N) is in eastern China and at the western end of the Yangtze River Delta. It is a strategic dual-node city of the “Belt and Road Initiative” (Chan et al. 2019) and the Yangtze River Economic Belt (YREB) (Zhang et al. 2021) (Fig. 1). Located in the subtropical monsoon humid climate, the surface water resources are abundant. The main water systems are the Huaihe River Basin and the Yangtze River, and there are lakes/reservoirs of different sizes in the urban area and its surroundings, with a total water area of ~824 km^2. The ecological environment value is very high.

As the capital of Anhui Province and characterized by rapid economic development, the urban area of Hefei has shown a significant expansion trend. High-density built-up urban areas and social and economic activities, along with climate change, have led to a serious urban heat-island effect (Liu et al. 2020). Therefore, Hefei is considered representative and has social significance, making it an appropriate area to research the cooling efficiency of urban lakes.

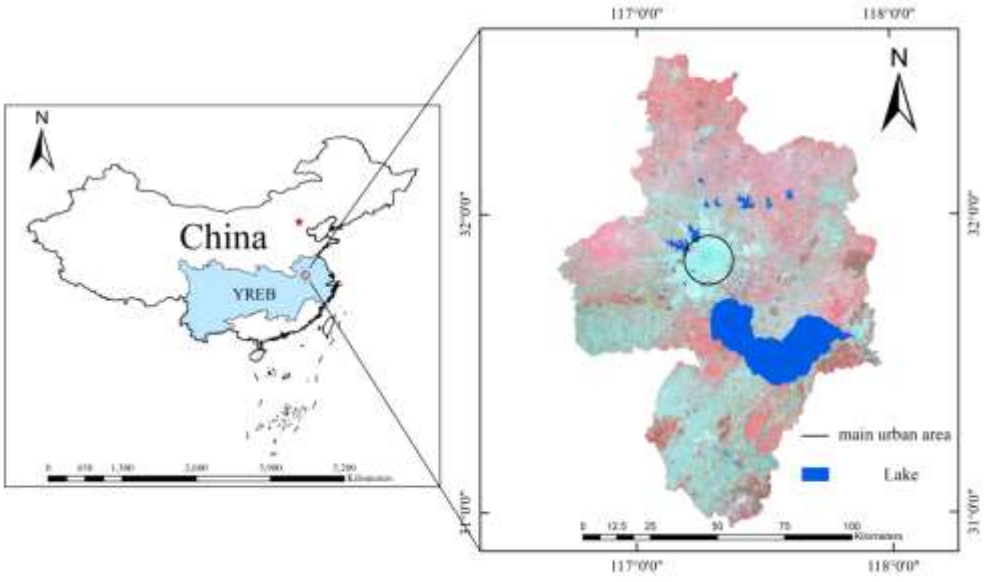

77 **Fig. 1 Study-area location and distribution of the lakes**

78 2.2 Data sources

79 For this study, information on lakes, land use, and surface temperature in Hefei were extracted from
80 Landsat remote-sensing images. All remote-sensing data were downloaded from the China Geospatial
81 Data Cloud website (website: http://www.gscloud.cn). For this research, we selected four scenes of
82 Landsat remote-sensing data (April 14, 2005; April 28, 2010; May 12, 2015; and April 15, 2020) acquired
83 during clear weather (0% cloud coverage). After preprocessing (such as radiometric calibration,
84 atmospheric correction, and image fusion), we applied surface-temperature inversion and land-use-type
85 classification.

86 In this study, to explore the factors influencing thermal mitigation in urban lakes, we selected 17
87 lakes with areas in the range 0.16–775.94 km^2 and distributed in and surrounding the main urban areas, as
88 interpreted from water data (Fig. 1). Among them, six lakes (including Nanyan, Swan, Feicui Lakes, etc.)
89 are relatively close to the city center, where they are surrounded by tall, densely situated buildings and
90 where social and economic activities are concentrated; the other 11 lakes, which are relatively far away
91 from the city center, are surrounded by a good ecological environment and scattered built land.

92 2.3 Research methods

93 2.3.1 Land-use-type extraction and urban-center analysis

94 Using Landsat remote-sensing images, we extracted Hefei land-use types in 2005, 2010, 2015, and
95 2020 by using ArcGIS 10.2 supervised classification, which divided the data into four main classes: water
96 and three land categories (built land, woodland, and other). Using the ArcGIS 10.2 software, we extracted
97 the built land with the largest area and determined its geometric center to represent the city center. We also

98 determined the geometric center of each lake, which we then used to derive the distance from each lake to
99 the city center.

100 **2.3.2 Water-information extraction and surface-temperature inversion**

101 Commonly used waterbody indices are the Normalized Difference Water Index (NDWI) (Teng et al.
102 2021) and the Modified Normalized Difference Water Index (MNDWI) (Bakr and Abd El-kawy 2020). In
103 this study, to extract water information, we used the MNDWI formula:

104 $$MNDWI = \frac{\rho_{Green} - \rho_{MIR}}{\rho_{Green} + \rho_{MIR}} \quad (1)$$

105 where ρ_{Green} represents the reflectance in the green band, and ρ_{MIR} represents the reflectance in the
106 mid-wave infrared band.

107 The surface-temperature inversion algorithms include mainly the radiative-transfer equation (Yao et
108 al. 2020), the single-channel algorithm (Sahani 2021), and the split-window algorithm (Zarei et al. 2021).
109 The radiative-transfer equation method has a wide range of applicability and can be applied to
110 thermal-infrared remote-sensing data from any sensor (Sekertekin 2019). In this study, we used the
111 radiative-transfer equation method for ground-temperature inversion. The thermal-infrared radiance value
112 received by the satellite sensor L_λ includes the energy of the surface radiance reaching the satellite
113 sensor after attenuation by the atmosphere, the upward radiance of the atmosphere, and the energy of the
114 downward radiance of the atmosphere reaching the satellite sensor after being reflected by the ground
115 (Cheng et al. 2021; Chan et al. 2021). The formula can be written as

116 $$\mathrm{L}_\lambda = \left[\varepsilon B\left(T_s\right) + \left(1-\varepsilon\right) L\downarrow\right]\tau + L\uparrow \quad (2)$$

117 Where ε is land-surface emissivity, T_S is real surface temperature (in K units), $B\left(T_S\right)$ is brightness

118 temperature, $L\downarrow$ is downward atmospheric radiance, $L\uparrow$ is upward atmospheric radiance, and τ is
119 transmittance of thermal-infrared band in the atmosphere.

120 **2.3.3 Spatial analysis of lake-cooling effect**

121 Applying the ArcGIS 10.2 spatial-analysis tool to Hefei land-use type and surface-temperature data,
122 we generated the boundaries of each lake and buffer zones at 60-m intervals. We used the 85 resulting
123 multilevel buffer zones to explore the cooling effect of urban lakes on the surrounding environment.
124 Using the ArcGIS 10.2 zonal-statistics tool to determine the mean surface temperature in each buffer zone,
125 we drew the surface-temperature change curve for each land-use type.

126 In this study, to weaken the influence of the synergistic cooling effect of woodland, grassland, and
127 water, we considered the cooling effect of lakes only on built land. Accordingly, we define cooling
128 intensity by the difference between the first turning point on the temperature curve of the built land and
129 the central temperature of lake (Mandal et al. 2022) (Eq. 3) and the cooling distance (D_L) by the buffer
130 distance corresponding to the first turning point on the temperature curve of the built land (Du et al. 2016)
131 (Fig. 2). Shorter distances to the lakes correspond to stronger cooling effects. When the distance reaches a
132 certain threshold, the surface temperature of various land-use types tends to stabilize, as the cooling
133 efficiency of the lake gradually dissipates. The lake-cooling-intensity efficiency refers to the cooling
134 intensity of the lake per unit area, and the cooling-distance efficiency refers to the cooling distance of the
135 lake per unit area.

136 Cooling intensity is as

137 $$I_L = T_B - T_L \tag{3}$$

138 Where T_B is the mean surface temperature of built land at the first turning point, T_L is the mean

central temperature of lake, and I_L is the corresponding cooling intensity.

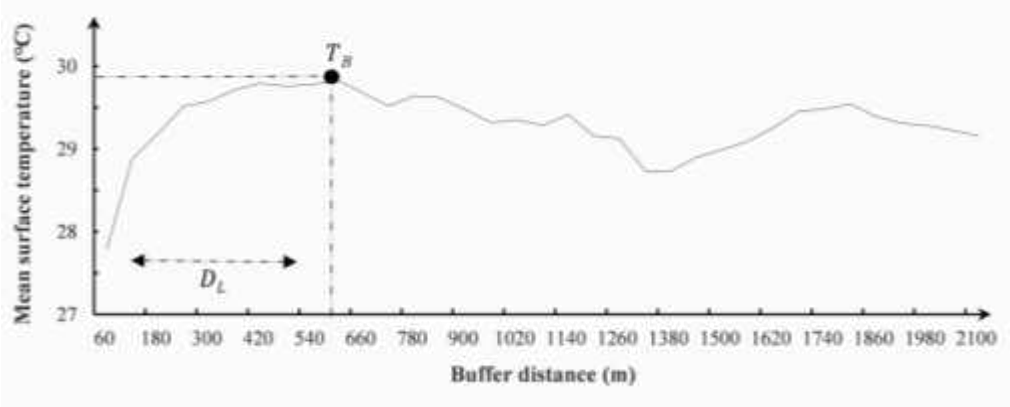

Fig. 2 Conceptual curve of cooling intensity and cooing distance

3 Analysis of results

3.1 Urban expansion and urban heat-island changes during 2005–2020

In this study, we used supervised classification to map Hefei land-use types into three different categories (built land, woodland, and other) and water for the years 2005, 2010, 2015, and 2020 (Fig. 3). Then we evaluated the accuracy of the resulting classification and tabulated the overall accuracy and Kappa coefficients (Table 1). The Kappa coefficients were all >0.85, and the classification results met the needs of our subsequent research.

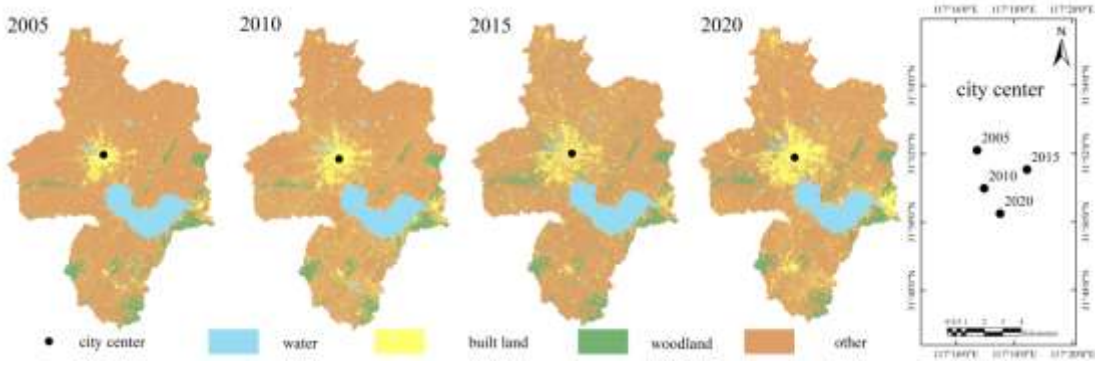

Fig. 3 Land-use-type map of Hefei during 2005–2020

Table 1 Supervised-classification accuracy and built-area change for Hefei during 2005–2020

Date	Classification accuracy	Kappa coefficient	Built area (km^2)
April 14, 2005	85.76%	0.88	225
April 28, 2010	86.23%	0.89	326
May 12, 2015	85.15%	0.86	416
April 15, 2020	87.34%	0.87	481

Built areas expanded over time from 225 km^2 in 2005 to 481 km^2 in 2020 (Fig. 3 and Table 1). Although the mean annual expansion rate during 2005–2020 was 5.20%, it reached 9.00% during 2005–2010. At the same time, the location of the city center changed continuously, gradually shifting to the southeast during 2005–2020.

According to the radiative-transfer equation method (Section 2.3), the land-surface temperature of Hefei inverted during 2005–2020, as shown by changes in its spatial distribution (Fig. 4).

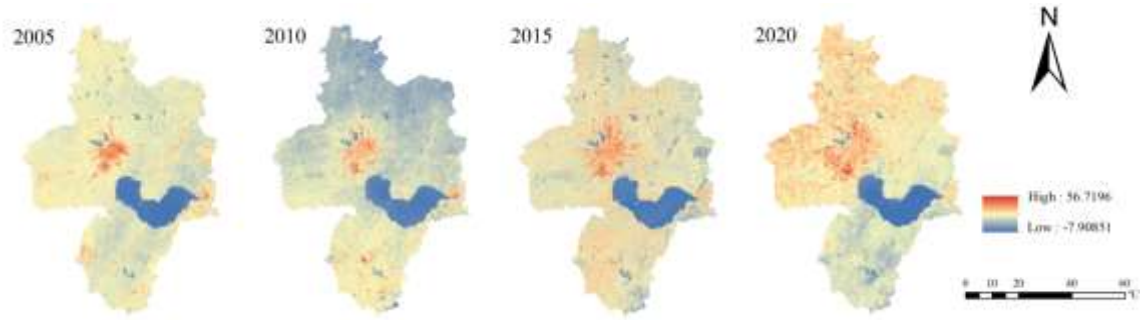

Fig. 4 Land-surface temperature in Hefei, 2005–2020

Representing a significant heat-island phenomenon, the temperature of the built land is significantly higher than that of the surrounding areas (Fig. 4). Among them, owing to the rainfall on April 28, 2010, the mean surface temperature was low. During 2005–2020, the built area increased from 225 km^2 to 481

163 km^2, and the area of the heat island gradually increased with the expansion of the city.

164 To further analyze the spatiotemporal heterogeneity of land-surface temperature in the study area, we
165 determined the mean surface temperature of different land-use types in the main urban area of four-phase
166 multispectral remote-sensing images during 2005–2020 (Table 2).

167 **Table 2 Mean surface temperatures for different land-use types in Hefei's main urban area of four-phase**
168 **multispectral remote-sensing images during 2005–2020**

	Mean surface temperature (°C)			
Date	Built land	Water	Woodland	Other
April 14, 2005	26.35	16.24	24.14	23.60
April 28, 2010	22.85	16.82	19.77	20.61
May 12, 2015	31.43	20.11	25.78	29.51
April 15, 2020	29.63	18.83	26.26	27.53

169 The mean surface temperatures of the main urban areas in 2005, 2010, 2015, and 2020 were 22.58°C,
170 20.01°C, 26.71°C, and 25.56°C, respectively. During 2005–2020, the mean surface temperature of
171 different land-use types in the main city showed an upward trend, and the urban heat-island effect
172 gradually increased (Table 2). The land-use type corresponding to the maximum mean surface
173 temperature is built land, and that corresponding to the minimum value is water.

174 3.2 Analysis of cooling efficiency of different lakes

175 To analyze the temporal and spatial differences in the cooling efficiency of different lakes, we

176 determined lake area and central temperature of lake, distance from the lake to the city center, and cooling
177 efficiency of 17 lakes in 2005, 2010, 2015, and 2020, including Ziyun, Swan, Chaohu Lakes, etc (Table
178 A1).

179 **Table 3 Statistics of cooling-efficiency index of 17 lakes during 2005–2020**

Year	Center temperature of all lakes (°C)		Cooling intensity (°C)		Cooling distance (m)		Cooling-intensity efficiency (°C/km^2)		Cooling-distance efficiency (m/km^2)	
	mean	interval	mean	interval	mean	interval	mean	interval	mean	interval
2005	18.25	15.41–20.42	7.51	5.21–10.74	508.24	120–960	9.73	0.01–21.25	645.65	1.22–1714.29
2010	17.40	15.39–18.87	4.44	2.23–6.41	525.88	120–1080	6.80	0.01–26.68	797.92	1.36–4434.78
2015	20.87	18.87–22.10	9.43	8.15–11.02	431.25	120–840	11.98	0.01–36.61	512.85	0.75–1411.76
2020	21.48	16.97–23.06	8.93	6.71–11.18	441.18	120–1140	12.79	0.01–34.82	546.82	1.44–2086.96

180 These results show that during 2005–2020, under the influence of urban expansion and the
181 intensification of the heat-island effect, the mean central temperature, cooling intensity, and
182 cooling-intensity efficiency of the lakes showed an increasing trend and significant spatial and temporal
183 heterogeneity, whereas the mean cooling distance and cooling-distance efficiency showed a decreasing
184 trend.

185 ## 3.3 Factors influencing cooling efficiency of different lakes

186 To explore spatiotemporal factors influencing the cooling efficiency of different lakes, we used SPSS
187 (Version 22) software to analyze correlation among lake area, central temperature of lake, distance from

the lake to the city center, and cooling efficiency (Table 4).

Table 4 Correlation among lake area, central temperature of lake, distance from lake to city center, and cooling efficiency

	Cooling intensity (°C)	Cooling distance (m)	Cooling-intensity efficiency (°C/km^2)	Cooling-distance efficiency (m/km^2)
Lake area (km^2)	0.18	0.49*	−0.29**	−0.24
Central temperature of lake (°C)	0.55*	−0.28**	0.62*	0.27**
Distance from lake to city center (km)	−0.15	−0.02	−0.37*	−0.46*

* Significant correlation at the 0.01 level (two-tailed).

** Significant correlation at the 0.05 level (two-tailed).

According to our data (Table 4), the lake-cooling intensity and distance strongly correlate with lake area and central temperature of lake but weakly correlate with the distance from the lake to the city center; the cooling intensity and central temperature of lake are positively correlated ($R = 0.55$, $P < 0.01$). Thus, for a given lake, the higher its central temperature, the stronger the cooling intensity. Also, the cooling distance is positively correlated with the lake area ($R = 0.49$, $P < 0.01$); the larger the lake, the greater the cooling distance. The central temperature of lake and cooling distance are negatively correlated ($R = -0.28$, $P < 0.05$); as the central temperature of lake decreases, the cooling distance shows an increasing trend.

The lake-cooling-intensity and cooling-distance efficiencies are strongly influenced by lake area, central temperature of lake, and distance from the lake to the city center. The cooling-intensity efficiency is negatively correlated with lake area ($R = -0.29$, $P < 0.05$): the larger the lake, the lower the cooling-intensity efficiency. The cooling-intensity efficiency has a positive correlation with the central temperature of lake ($R = 0.62$, $P < 0.01$): the higher that temperature, the higher the cooling-intensity efficiency. The cooling-intensity efficiency is negatively correlated with the distance from the lake to the city center ($R = -0.37$, $P < 0.01$): the greater that distance, the lower the cooling-intensity efficiency. The cooling-distance efficiency is positively correlated with the central temperature of lake ($R = 0.27$, $P < 0.05$): the greater that temperature, the higher the cooling-distance efficiency. The cooling-distance efficiency is negatively correlated with the distance from the lake to the city center ($R = -0.46$, $P < 0.01$): the greater that distance, the lower the cooling-distance efficiency.

To further study the effect of lake area on its cooling intensity and distance, and to explore the response of cooling efficiency to urban expansion, we performed regression analysis on the size of 17 selected lakes in Hefei and their cooling efficiency (Fig. 5).

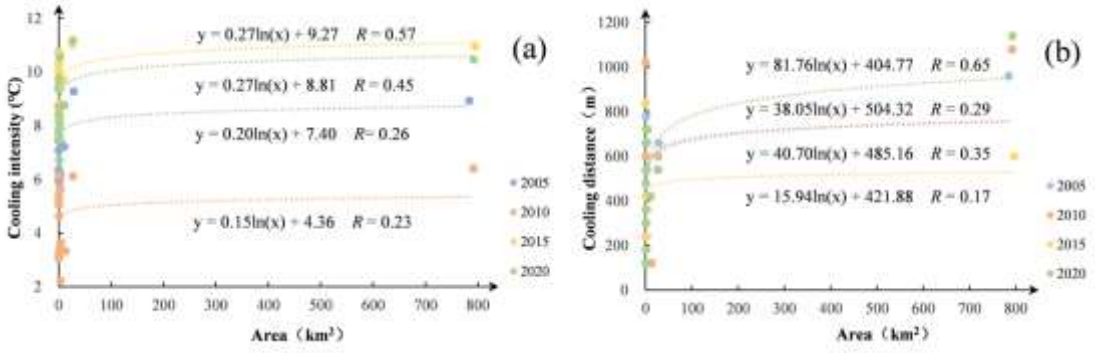

Fig. 5 Regression relationships between (a) lake area and cooling intensity, and (b) lake area and cooling distance

We found that during 2005–2020, there was a positive logarithmic relationship among cooling intensity, cooling distance, and the lake area (Fig. 5). Accordingly, as the lake area increased, the cooling

intensity and distance gradually increased. Above a certain threshold, the cooling intensity tends to stabilize. This effect is consistent with previous conclusions that the cooling efficiency of lakes depends to a large extent on the size of the lake; related studies have shown that when the area of the lake is less than 1 hectare, the compact shape can exert its cooling efficiency more effectively (Yang et al. 2020).

4 Discussion

4.1 Influence of different lake locations on cooling efficiency

4.1.1 Cooling effect of lakes in main urban area

According to their distance from the center of the main urban area of Hefei, we selected Nanyan, Swan, and Feicui Lakes and Wangzui, Dongpu + Dafangying, and Baiyanba Reservoirs to represent lakes in the main urban area. The distribution interval of the distance of these waterbodies from the city center is 8.45–16.65 km, and they have the mean area of 5.13 km^2. We analyzed these six waterbodies to derive a quantitative relationship between lake size in the main urban area and cooling efficiency during 2005–2020 (Fig. 6).

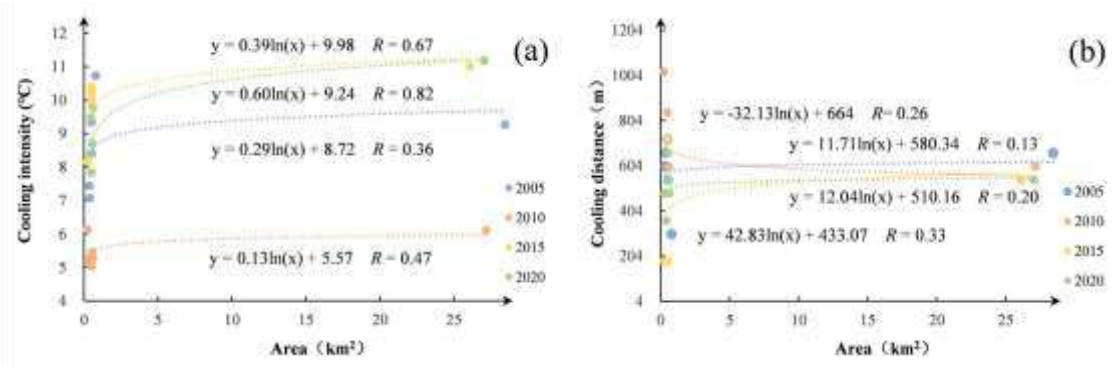

Fig. 6 Cooling efficiency of lakes in main urban area. (a) cooling intensity; (b) cooling distance

We found a positive logarithmic relationship between the cooling efficiency and lake size in the main urban area (Fig. 6). That is, the cooling intensity and distance increase with the lake size. During 2005–

2020, the mean cooling intensity was 8.71°C, 5.55°C, 9.97°C, and 9.23°C, and the mean cooling distance was 580, 670, 432, and 510 m. Accordingly, under the influence of the heat-island effect, the mean cooling intensity basically shows an upward trend, and the mean cooling distance, a downward trend.

4.1.2 Cooling effect of lakes surrounding main urban area

According to the statistical distance from the waterbody to the center of the main urban area of Hefei, we selected Ziyun and Chaohu Lakes and Yiwan, Xiegaotang, Tanchong, Zhangqiao, Luoji, Caitang, Guanwan, Miaoji, and Zhongxing Reservoirs as representative of the lakes around the main urban area, with the mean area of 74.16 km^2. We analyzed the correlation between lake area and cooling efficiency during 2005–2020 (Fig. 7).

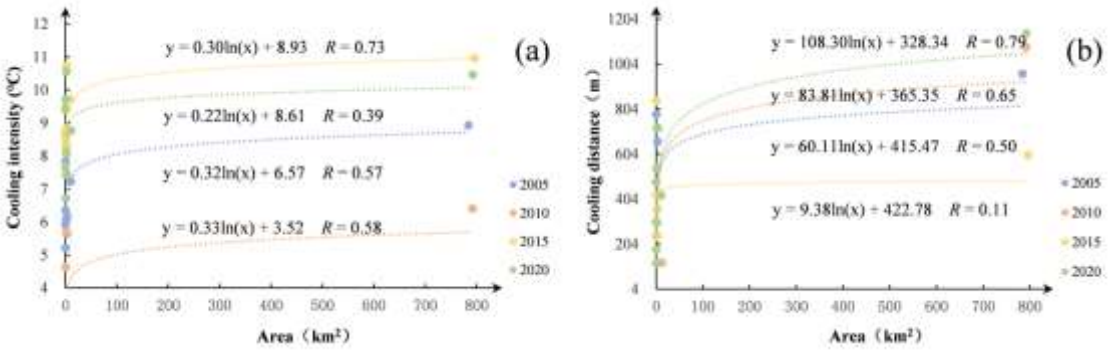

Fig. 7 Cooling efficiency of lakes surrounding main urban area. (a) cooling intensity; (b) cooling distance

We found a positive logarithmic relationship between the cooling efficiency and the area of lakes surrounding the main urban area (Fig. 7). The trends of the cooling intensity and the cooling distance of these lakes are the same as those in the main urban area. During 2005–2020, the mean cooling intensity was 6.86°C, 3.84°C, 9.19°C, and 8.76°C, and the mean cooling distance was 469.09, 447.27, 430.91, and 403.64 m. The main reason these intensity and distance values for lakes surrounding the main urban area are smaller than for those in the main urban area is that they are farther away from the main urban area

where the heat-island effect is most concentrated, and their ability to absorb the high surface temperature caused by the heat-island effect is limited. In future urban planning, to effectively alleviate such heat-island effects, the optimal configuration of the internal landscape of the main urban area needs to be the main consideration, and it can be achieved mainly by the adjustment of lake area.

4.1.3 Relationship between distance from lake to city center and cooling efficiency

According to the above analysis on the cooling effect of lakes in and surrounding the main urban areas, there was a strong correlation between the distance from the lake to the city center and the cooling efficiency. Therefore, we analyzed data from 2005–2020 to derive the quantitative relationship between the cooling-intensity efficiency, cooling-distance efficiency, and the distance from the lake to the city center (Fig. 8).

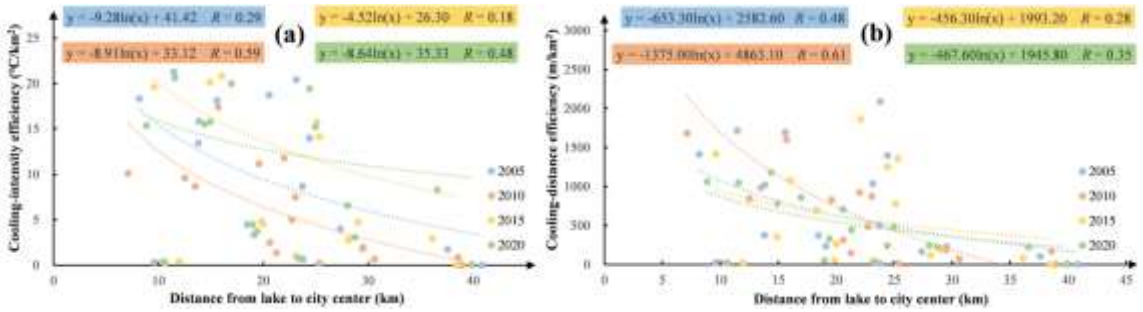

Fig. 8 Correlation between distance from lake to city center and cooling efficiency.

(a) cooling-intensity efficiency; (b) cooling-distance efficiency

We found negative logarithmic relationships among the cooling-intensity and cooling-distance efficiencies and the distance from the lake to the city center (Fig. 8). Accordingly, as the distance from the lake to the city center increased, the cooling-intensity and cooling-distance efficiencies decreased. The main cause is the temperature difference between the lake and objects on the surrounding land. That is, the greater the distance of the lake to the city center, the smaller the ground-temperature difference and the

weaker the water's ability to absorb heat effects that are accompanied by corresponding reductions in cooling-intensity and cooling-distance efficiencies.

4.2 Response of lake-cooling efficiency to urban expansion

According to the above results, as the distance from the lake to the city center decreased, the cooling effect of the lake became prominent. Therefore, we selected the mean central temperature of the lakes in the main urban area and built size as the indicators to further analyze the response of lake-cooling efficiency to urban expansion.

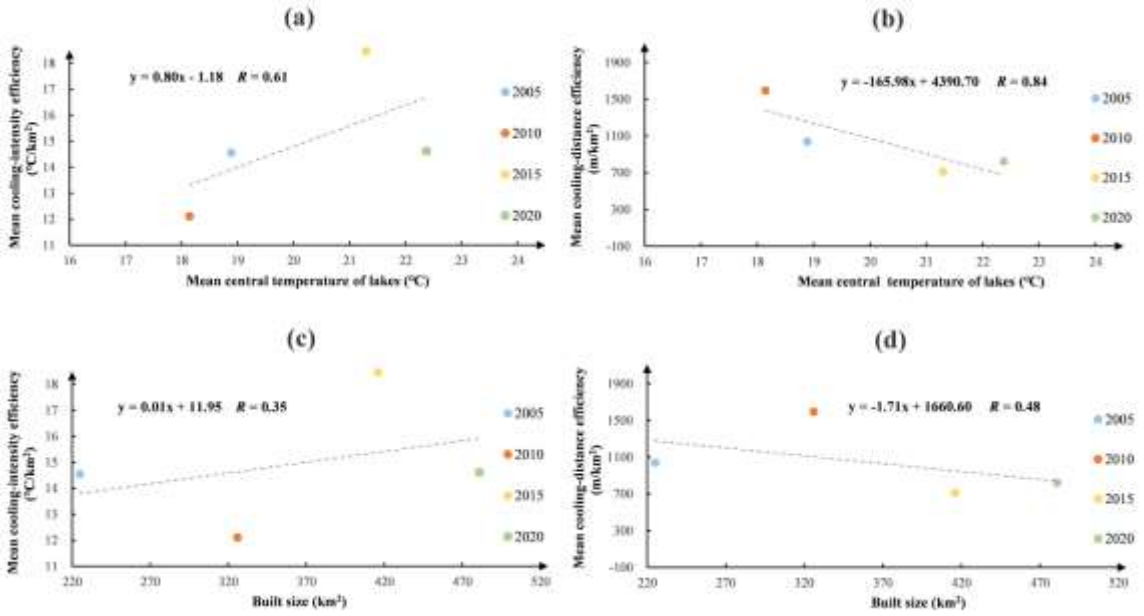

Fig. 9 The mean central temperature of lakes vs mean cooling-intensity efficiency(a), and vs mean cooling-distance efficiency(b); the built size vs mean cooling-intensity efficiency(c), and vs mean cooling-distance efficiency(d).

During 2005–2020, with the expansion of the main urban area of Hefei and the intensification of the heat-island effect, the mean cooling-intensity efficiency of the lakes in the main urban area increased with the increase in the built size and mean central temperature of lakes, but the mean

cooling-distance efficiency decreased accordingly (Fig. 9). The main cause is that the lakes in the main urban area are in the concentrated heat-island effect, and the temperature difference between the lakes and urban built area is considerable. Thus, the cooling effect is obvious, and the cooling intensity of the lakes per unit area increases with intensifying heat-island effect. However, because the size of the lakes in the main urban area is small (with a mean area of 5.13 km^2), and with the increase in the central temperature of the lakes caused by the heat-island effect, the cooling distance of the lakes per unit area decreases.

5 Conclusions

In this study, we analyzed and compared the cooling efficiency of different lakes in and surrounding the main urban areas of Hefei, China. We analyzed the factors influencing lake-cooling efficiency from the aspects of lake size and location, and we explored the response of lake-cooling efficiency to urban expansion. According to the results of this study, the following conclusions can be drawn:

(1) Cooling intensity was positively correlated with the central temperature of the lakes ($R = 0.55$, $P < 0.01$), and cooling distance was negatively correlated with the central temperature of the lakes ($R = -0.28$, $P < 0.05$). As the central temperature of the lakes increased gradually, cooling intensity increased significantly and cooling distance decreased.

(2) Lake area was significantly positively correlated with cooling distance ($R = 0.49$, $P < 0.01$) and weakly positively correlated with cooling intensity. As lake area increased, cooling intensity and distance also increased. However, when lake area reached a certain threshold, cooling intensity tended to stabilize.

(3) At the greater distances of the lakes from the city center, cooling-intensity and cooling-distance efficiencies were lower. This was mainly because the surrounding lakes were far from the main urban area

where the heat-island effect was the strongest, and the absorption capacity of the surface-heat radiation caused by the heat-island effect was limited. Further, mean cooling intensity and distance were smaller than those of the lakes in the main urban area.

(4) With enlarging city scale and aggravating heat-island effect from 2005 to 2020, the cooling-intensity efficiency of the lakes in the main urban area gradually increased, whereas the cooling-distance efficiency of the lakes decreased.

Ethical approval and consent to participate: Not applicable

Consent for publication: Not applicable

Author information

Affiliations: [a] School of Science, Anhui Agricultural University, Hefei, Anhui 230036, China

[b] Key Laboratory of Agricultural Sensors, Ministry of Agriculture and Rural Affairs of China, Hefei, Anhui 230036, China

Lin Xuening, Cui Yuhuan, Hao Shuang, Hong Hong, Zhang Man, Zhang Jingdong, Li Ruonan, Liu Mengyu

Author contribution: Conceptualization: Cui Yuhuan; Methodology: Hao Shuang; Software: Lin Xuening, Hong Hong, and Zhang Man; Validation: Zhang Jingdong, Li Ruonan, and Liu Mengyu; Formal analysis: Cui Yuhuan; Investigation: Hong Hong and Zhang Man; Resources: Zhang Jingdong, Li Ruonan, and Liu Mengyu; Data curation: Lin Xuening; Writing—original draft preparation: Lin Xuening; Writing—review and editing: Cui Yuhuan; Visualization: Hong Hong; Supervision: Cui Yuhuan; Project administration: Cui Yuhuan; Funding acquisition: Cui Yuhuan and Hao Shuang.

All authors have read and agreed to the published version of the manuscript.

Funding: This research was funded by the National Natural Science Foundation of China (grant numbers 32171573 and 41801332) and Anhui University Natural Science Research Project (KJ2021A0178).

Conflicts of Interest: The authors declare no conflict of interest.

Data availability: Data and material access are not available.

References

Bakr N, Abd El-kawy OR (2020) Modeling the artificial lake-surface area change in arid agro-ecosystem: A case study in the newly reclaimed area, Egypt. Journal of Environmental Management 271:110950. https://doi.org/10.1016/j.jenvman.2020.110950

Cai Z, Han GF, Chen MC (2018) Do water bodies play an important role in the relationship between urban form and land surface temperature? Sustainable Cities and Society 39:487–498. https://doi.org/10.1016/j.scs.2018.02.033

Chan HK, Dai J, Wang XJ et al (2019) Logistics and supply chain innovation in the context of the Belt and Road Initiative (BRI). Transportation Research Part E: Logistics and Transportation Review 132:51–56. https://doi.org/10.1016/j.tre.2019.10.009

Chan HP, Konstantinou KI, Blackett M (2021) Spatio-temporal surface temperature variations detected by satellite thermal infrared images at Merapi volcano, Indonesia. Journal of Volcanology and Geothermal Research 420:107405. https://doi.org/10.1016/j.jvolgeores.2021.107405

Chen M, Dai F, Yang B, Zhu SW (2019) Effects of neighborhood green space on $PM_{2.5}$ mitigation: Evidence from five megacities in China. Building and Environment 156:33–45. https://doi.org/10.1016/j.buildenv.2019.03.007

Chen XT, Wang ZT, Bao Y (2021) Cool island effects of urban remnant natural mountains for cooling communities: A case study of Guiyang, China. Sustainable Cities and Society 71:102983. https://doi.org/10.1016/j.scs.2021.102983

345 Cheng J, Meng XC, Dong SY et al (2021) Generating the 30-m land surface temperature product over continental China and USA from landsat 5/7/8
346 data. Science of Remote Sensing 4:100032. https://doi.org/10.1016/j.srs.2021.100032

347 Cheval S, Popa AM, Sandric I, Ioja IC (2020) Exploratory analysis of cooling effect of urban lakes on land surface temperature in Bucharest
348 (Romania) using Landsat imagery. Urban Climate 34:100696. https://doi.org/10.1016/j.uclim.2020.100696

349 Douglas ANJ, Irga PJ, Torpy FR (2019) Determining broad scale associations between air pollutants and urban forestry: A novel multifaceted
350 methodological approach. Environmental Pollution 247:474–481. https://doi.org/10.1016/j.envpol.2018.12.099

351 Du HY, Song XJ, Jiang H, Kan ZH, Wang ZB, Cai YL (2016) Research on the cooling island effects of water body: A case study of Shanghai, China.
352 Ecological Indicators 67:31–38. https://doi.org/10.1016/j.ecolind.2016.02.040

353 Fan SX, Li XP, Han J, Cao Y, Dong L (2017) Field assessment of the impacts of landscape structure on different-sized airborne particles in
354 residential areas of Beijing, China. Atmospheric Environment 166:192–203. https://doi.org/10.1016/j.atmosenv.2017.07.026

355 Gunawardena KR, Wells MJ, Kershaw T (2017) Utilising green and bluespace to mitigate urban heat island intensity. Science of The Total
356 Environment 584-585:1040–1055. https://doi.org/10.1016/j.scitotenv.2017.01.158

357 Janhall S (2015) Review on urban vegetation and particle air pollution – Deposition and dispersion. Atmospheric Environment 105:130–137.
358 https://doi.org/10.1016/j.atmosenv.2015.01.052

359 Ke XL, Men HL, Zhou T et al (2021) Variance of the impact of urban green space on the urban heat island effect among different urban functional
360 zones: A case study in Wuhan. Urban Forestry & Urban Greening 62:127159. https://doi.org/10.1016/j.ufug.2021.127159

361 Liu X, Zhou YY, Yue WZ et al (2020) Spatiotemporal patterns of summer urban heat island in Beijing, China using an improved land surface
362 temperature. Journal of Cleaner Production 257:120529. https://doi.org/10.1016/j.jclepro.2020.120529

363 Mandal J, Patel PP, Samanta S (2022) Examining the expansion of Urban Heat Island effect in the Kolkata Metropolitan Area and its vicinity using
364 multi-temporal MODIS satellite data. Advances in Space Research 69(5):1960–1977. https://doi.org/10.1016/j.asr.2021.11.040

365 Matos P, Vieira J, Rocha B, Branquinho C, Pinho P (2019) Modeling the provision of air-quality regulation ecosystem service provided by urban
366 green spaces using lichens as ecological indicators. Science of The Total Environment 665:521–530. https://doi.org/10.1016/j.scitotenv.2019.02.023

367 Moss JL, Doick KJ, Smith S, Shahrestani M (2019) Influence of evaporative cooling by urban forests on cooling demand in cities. Urban Forestry &
368 Urban Greening 37:65–73. https://doi.org/10.1016/j.ufug.2018.07.023

369 Sahani N (2021) Assessment of spatio-temporal changes of land surface temperature (LST) in Kanchenjunga Biosphere Reserve (KBR), India using
370 Landsat satellite image and single channel algorithm. Remote Sensing Applications: Society and Environment 24:100659.
371 https://doi.org/10.1016/j.rsase.2021.100659

372 Santamouris M (2020) Recent progress on urban overheating and heat island research. Integrated assessment of the energy, environmental,
373 vulnerability and health impact. Synergies with the global climate change. Energy and Buildings 207:109482.
374 https://doi.org/10.1016/j.enbuild.2019.109482

375 Sekertekin A (2019) Validation of Physical Radiative Transfer Equation-Based Land Surface Temperature Using Landsat 8 Satellite Imagery and
376 SURFRAD in-situ Measurements. Journal of Atmospheric and Solar-Terrestrial Physics 196:105161. https://doi.org/10.1016/j.jastp.2019.105161

377 Teng JK, Xia SX, Liu Y, Yu XB, Duan HL, Xiao H, Zhao CP (2021) Assessing habitat suitability for wintering geese by using Normalized
378 Difference Water Index (NDWI) in a large floodplain wetland, China. Ecological Indicators 122:107260.
379 https://doi.org/10.1016/j.ecolind.2020.107260

380 von Schneidemesser E, Steinmar K, Weatherhead EC, Bonn B, Gerwig H, Quedenau J (2019) Air pollution at human scales in an urban environment:
381 Impact of local environment and vehicles on particle number concentrations. Science of The Total Environment 688:691–700.
382 https://doi.org/10.1016/j.scitotenv.2019.06.309

383 Wang ZH (2022) Reconceptualizing urban heat island: Beyond the urban-rural dichotomy. Sustainable Cities and Society 77:103581.
384 https://doi.org/10.1016/j.scs.2021.103581

Wu W, Li LD, Li CL (2021) Seasonal variation in the effects of urban environmental factors on land surface temperature in a winter city. Journal of Cleaner Production 299:126897. https://doi.org/10.1016/j.jclepro.2021.126897

Yang GY, Yu ZW et al (2020) How can urban blue-green space be planned for climate adaption in high-latitude cities? A seasonal perspective. Sustainable Cities and Society 53:101932. https://doi.org/10.1016/j.scs.2019.101932

Yao L, Li T, Xu MX, Xu Y (2020) How the landscape features of urban green space impact seasonal land surface temperatures at a city-block-scale: An urban heat island study in Beijing, China. Urban Forestry & Urban Greening 52:126704. https://doi.org/10.1016/j.ufug.2020.126704

Yao X, Yu KY, Zeng XJ et al (2022) How can urban parks be planned to mitigate urban heat island effect in "Furnace cities"? An accumulation perspective. Journal of Cleaner Production 330:129852. https://doi.org/10.1016/j.jclepro.2021.129852

Zarei A, Shah-Hosseini R, Ranjbar S, Hasanlou M (2021) Validation of non-linear split window algorithm for land surface temperature estimation using Sentinel-3 satellite imagery: Case study; Tehran Province, Iran. Advances in Space Research 67(12):3979–3993. https://doi.org/10.1016/j.asr.2021.02.019

Zhang YY, Sun MY, Yang RJ et al (2021) Decoupling water environment pressures from economic growth in the Yangtze River Economic Belt, China. Ecological Indicators 122:107314. https://doi.org/10.1016/j.ecolind.2020.107314

Zheng YM, He YR, Zhou Q, Wang HW (2022) Quantitative Evaluation of Urban Expansion using NPP-VIIRS Nighttime Light and Landsat Spectral Data. Sustainable Cities and Society 76:103338. https://doi.org/10.1016/j.scs.2021.103338

Supplementary Files

This is a list of supplementary files associated with this preprint. Click to download.

- SupplementaryMaterial.docx